

Shaping of Neurons by Environmental Interaction

Artur Luczak

Abstract The geometry of dendritic trees plays an important role in determining the connectivity. However, the extent to which environmental factors shape dendritic geometry remains largely unknown. Recent development of computational models can help us to better understand it. This chapter provides a description of one such model (Luczak, *J Neurosci Methods* 157:132–41, 2006). It demonstrates that assuming only that neurons grow in the direction of a local gradient of a neurotrophic substance, and that dendrites compete for the same resources, it is possible to reproduce the spatial embedding of major types of cortical neurons. In addition, this model can be used to estimate environmental conditions which shape actual neurons, as proposed in Luczak, *Front Comput Neurosci* 4:135, 2010. In summary, the presented model suggests that basic environmental factors, and the simple rules of diffusive growth can adequately account for different types of axonal and dendritic shapes.

1 Introduction

Saying that shape determines function is especially true for neurons. The shape of dendritic trees to a large degree determines electrophysiological properties of neurons (Migliore et al. 1995; Mainen and Sejnowski 1996; Krichmar et al. 2002) and neuronal connectivity (Amirikian 2005; Stepanyants and Chklovskii 2005; Cuntz et al. 2010; Perin et al. 2011). Experimental data suggests that both intrinsic and

A. Luczak (✉)

Department of Neuroscience, Canadian Centre for Behavioural Neuroscience,
University of Lethbridge, 4401 University Drive, Lethbridge, AB, Canada, T1K 3M4
e-mail: luczak@uleth.ca

23 extrinsic factors influence dendritic geometry, but the relative importance of those
24 factors is not well understood (Scott and Luo 2001). The complexity of interactions
25 between different intrinsic and extrinsic factors during the development of neuronal
26 arborization can make it very difficult to separate their contributions experimen-
27 tally. One of the approaches to address this question is to use computational model-
28 ing. Nevertheless, even with advances in computational neuroscience, it is not a
29 simple task, and it has taken decades to develop realistic models of neuronal growth.
30 For example, in its earliest works, only dendrograms were modeled (i.e., connectiv-
31 ity among branches and their length and diameter) yet spatial embedding or envi-
32 ronmental factors were not considered (Nowakowski et al. 1992; Van Pelt et al.
33 1997). In the later models of dendritic trees, 3D structures were included but with-
34 out considering environment. In these models, several parameters measured from
35 real neurons (e.g., the probability distribution of branching points as a function of
36 the distance from a soma) were used and stochastic procedures were applied to
37 recreate dendrites while disregarding influence of the environment (Ascoli 1999;
38 Burke and Marks 2002; Samsonovich and Ascoli 2003; Samsonovich and Ascoli
39 2005; Lindsay et al. 2007; Torben-Nielsen et al. 2008; Koene et al. 2009; for review
40 see Ascoli 2002).

41 In contrast to the above models based on statistical reconstruction of dendrites,
42 the most recent models can simulate 3D neuronal growth with incorporating external
43 factors. In these approaches, dendrite geometry parameters (e.g., number of
44 segments, branching probability, orientation) are not built into the model, but rather
45 geometry parameters emerge as a result of environmental factors such as the con-
46 centration of neurotropic factors, competition between neurons, and space limita-
47 tions (Luczak 2006; Zubler and Douglas 2009). External cues are well known to
48 play a significant role in shaping dendritic geometry (Horch and Katz 2002), and
49 hence these models account for the important biological processes underlying neu-
50 ronal geometry.

51 In this chapter, we focus on the model developed by Luczak (2006) which exam-
52 ines the effect of environmental factors on spatial embedding of neuronal trees. This
53 model is based on diffusion-limited aggregation (DLA), which is a well-established
54 physical model for the formation of structures controlled by diffusion processes
55 (Witten and Sander 1981). Prior research has demonstrated that DLA can provide a
56 good description of a variety of natural processes, such as electrical discharge in gas
57 (lightning) (Niemeyer et al. 1984), electrochemical deposition (Halsey 1990; Brady
58 and Ball 1984), or the growth of snowflakes (Family et al. 1987). The form of a typi-
59 cal DLA structure is illustrated in the insert of Fig. 1.

60 Previously, diffusive processes were invoked to explain the origin of dendritic
61 arbors by Hentschel and Fine (1996), who proposed a two-dimensional diffusion-
62 regulated model of dendritic morphogenesis in which cell growth depended upon
63 the local concentration of calcium. However, their model was restricted to only the
64 early stage of neuronal growth, and was based on *in vitro* dissociated cultures.
65 In order to generate a 3D embedding of fully developed dendritic trees, the present
66 model operates at a coarser level. It takes into account the local concentrations of
67 neurotrophic factors, but without including such details as changes in the concentra-
68 tions of ions along the dendrite membrane.

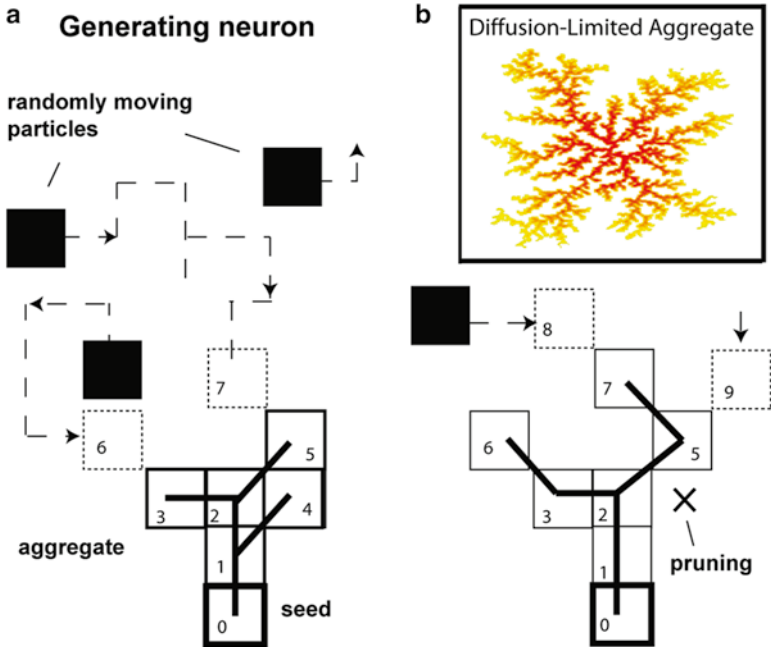


Fig. 1 Illustration of the DLA algorithm. (a) Randomly moving particles (*black*) stick irreversibly at their point of first contact with the aggregate (composed of particles 0–5). To each newly jointed particle, a parent particle is assigned and both become connected by a line segment. (b) While the aggregate grows, the particles at the terminals are randomly deleted from the aggregate (pruning) during a specified time window. Insert: Example of a two-dimensional DLA comprising 6,000 particles. The color intensity decreases in the order in which particles connected to the aggregate (reproduced from Luczak 2006 with permission from Elsevier)

2 Model Description

69

As described in details in (Luczak 2006), the growth rule for DLA can be defined inductively as follows: introduce a randomly moving particle at a large distance from an n -particle aggregate, which sticks irreversibly at its first point of contact with the aggregate, thereby forming an $n+1$ -particle aggregate. Figure 1a illustrates a sample trajectory of particles that stick to an aggregate composed of five particles (each particle is numbered in the order in which it contacts the aggregate; the seed particle is numbered 0). Stated differently, the aggregate grows by one step at the point of contact with a particle, thus prominent branches screen internal regions of the aggregate, preventing them from growing further (Halsey 1997). For computational efficiency, instead of one moving particle, m simultaneously moving particles were introduced (Voss 1984). For computational convenience, particles leaving box on one side, enter the box on the opposite side. In the presented model, the initial distribution of particles is a model parameter and thus particles are not always

70
71
72
73
74
75
76
77
78
79
80
81
82

83 uniformly distributed, which is a significant difference from the classical DLA.
84 As a result, there is a higher probability that the aggregate will have more branches
85 in areas with a higher concentration of particles.

86 A particle in the aggregate to which the new particle connects is called a parent
87 particle. When a new particle is connected to more than one particle in the aggre-
88 gate, the parent particle is selected at random. For example, in Fig. 1a, for particle
89 number 4, either particle number 1 or particle number 2 could be assigned as a par-
90 ent particle, and in this case, particle 1 was selected at random. Thus, the aggregate
91 is converted to a directed, acyclic graph (tree), where each particle becomes a node
92 connected by a segment to an assigned parent node.

93 Without additional restrictions, the aggregate would form a heavily branched
94 structure similar to the DLA in the insert of Fig. 1. Therefore, a pruning procedure
95 was implemented, which removes terminal particles from the aggregate. At each
96 iteration there is a probability p that any terminal particle of the aggregate can be
97 deleted if that particle was connected within the last s iterations, but later than five
98 iterations ago, where s is a pruning span parameter. As a result of the deletion, the
99 parent particle of the removed particle becomes again a terminal particle (eligible
100 for the deletion) unless it is a branching node. Thus, increasing pruning span
101 increases the number of deleted particles. Five iterations were chosen before apply-
102 ing pruning, primarily to allow for the initial growth of the aggregate. Nevertheless,
103 this parameter has a very minor effect on the geometry of a dendrite as compared to
104 pruning span. The removed particles do not return to the pool of particles, and the
105 seed particle cannot be removed by definition. The algorithm stops when no new
106 particle is connected for 100 iterations.

107 Illustration of the initial spatial distribution of particles for the granule cells is
108 presented in Fig. 2a. To eliminate tree variability due to seed position, the seed is
109 always located in the center at the bottom of the box, or when generating multiple
110 trees simultaneously, seeds are uniformly distributed at the bottom of the box. The
111 number of seed particles placed inside a box determined the number of aggregates.

112 The MATLAB code used to produce the described simulations is available upon
113 request, or it can be downloaded from: [http://lethbridgebraindynamics.com/
114 artur_luczak](http://lethbridgebraindynamics.com/artur_luczak).

115 3 Generating Different Neuronal Tree Types

116 The above description of how branching structures grow could be seen as an “innate”
117 set of rules which is the same for all neuronal types generated with this model. What
118 differentiates between growing a granule cell and a pyramidal cell in our model are
119 mostly differences in parameters defining environment. Interestingly, only two
120 environment factors were enough to define and reproduce diverse types of neuronal
121 trees. These factors were: the distribution of “neurotrophic particles” (NPs), and
122 space available to grow. Below we will describe in more detail the effect of both
123 factors on neuronal shape, beginning with the space constraints.

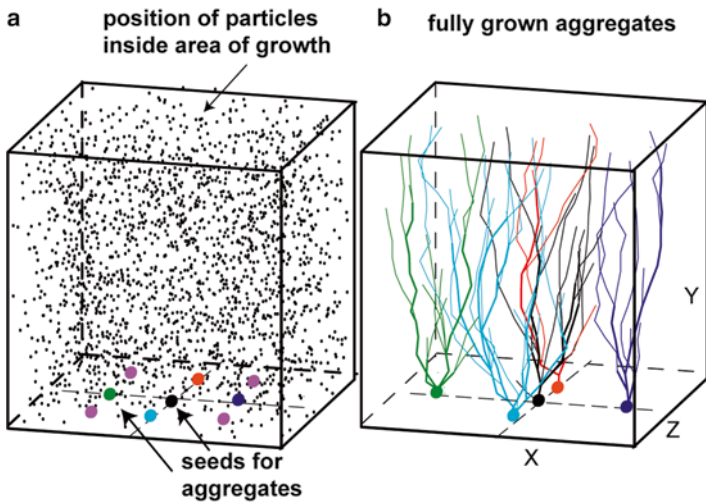


Fig. 2 Generating neurons in ensemble. (a) Illustration of the initial condition for generating nine aggregates. *Small black dots* denote initial location of NP particles. For illustration clarity only centers of NPs are marked, as the full size of NP used in this simulation ($\sim 10 \mu\text{m}$) would obstruct view of particles in the back. (b) Generated granule cells (cells in corners are not shown for visualization clarity). *Rectangular box* represents a space limitation imposed on the growth of aggregates (reproduced from Luczak 2006 with permission from Elsevier)

In our model, the shape of generated dendrites directly depends on the size of the rectangular box in which the neuron is growing (Fig. 2). For example, increasing the height–width ratio of the box changes the dendrite shape from that of a basal dendrite to a granule cell and, ultimately, to an apical dendrite. Decreasing relative width only in the Z-coordinate direction changes it from a basal dendrite to a Purkinje cell.

The use of a rectangular box to limit neuron growth may, at first sight, appear to impose an artificial constraint, whereas this actually simulates the space limitations imposed by the thickness of the cortical layers (height of the box), and by neighboring neurons growing simultaneously and competing for space and neurotrophic substances (length and width of the box) (Devries and Baylor 1997). For example, generating a neuron surrounded by other simultaneously growing cells resulted in a shape almost identical to growing this neuron in an isolated box with appropriately reduced size (Fig. 2). This is because the neighboring aggregates competed for available space and access to NPs, which limited the sideways growth of the neuron. Thus, sideways space limitation imposed in the model could also be viewed as another manifestation of constraints imposed by the spatial distribution of neurotrophic factors, where a neuron has a higher chance of getting access to NPs by extending its processes up rather than to the sides due to competition from other cells.

We found that it was also important to vary the distribution of NPs along the vertical direction to accurately reflect branching patterns of reproduced neurons.

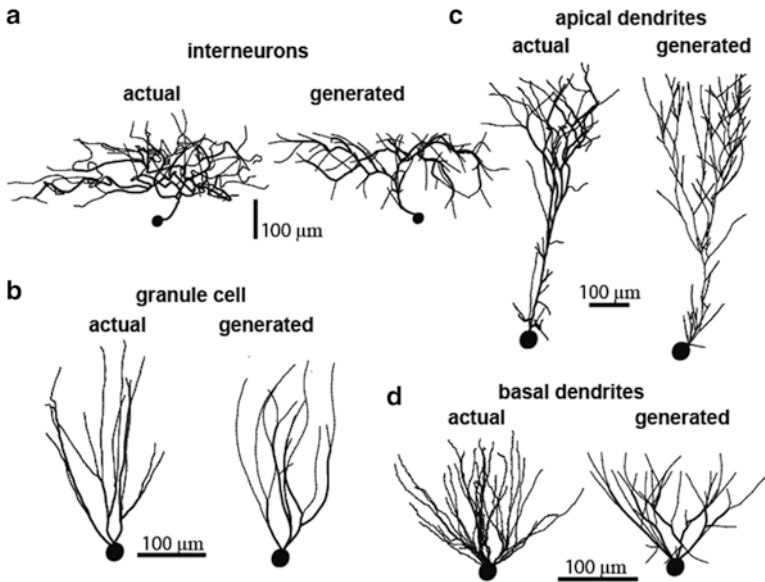


Fig. 3 Examples of real and generated neurons. **(a)** Examples of real and generated axonal trees of interneurons. **(b)** Examples of real and generated granule cells. **(c)** Examples of real and generated apical dendrites of pyramidal cells. **(d)** Examples of real and generated basal dendrites. For all neurons, the cell bodies are depicted by spheres (modified from Luczak 2006)

145 This at first was a surprise, but after examining the required patterns of NPs
 146 distribution, we found a striking similarity to the laminar structure of cortical layers.
 147 Thus, the difference in NPs concentration at different heights in the box could be a
 148 reflection of a different concentration of actual neurotrophic factors across different
 149 cortical layers. A direct consequence of “innate” properties of the DLA-based
 150 model is that increasing the concentration of NPs increases the density of branches.
 151 For example, increasing the concentration of NPs in the upper 30 % section of the
 152 box, while reducing it to almost zero elsewhere, produces an aggregate with the
 153 appearance of an interneuron (Fig. 3a) rather than of a granule cell or basal dendrite
 154 (Fig. 3b, d). As mentioned before, such changes in particle density along the vertical
 155 axis may be biologically justified as reflecting different cortical layers. In the model,
 156 the initial distribution of particle densities along the vertical axis exhibits a sharp
 157 transition between two regions with different concentrations. However, after a few
 158 iterations, the diffusive motion of NPs creates a smooth concentration gradient
 159 between the layers which is closer to real biological conditions. Due to much faster
 160 growth of the aggregate than diffusion of NPs between layers, the difference in
 161 concentration between layers is maintained throughout simulation. Thus, by chang-
 162 ing only the space available for growth, the spatial distribution of NPs (and the
 163 pruning span to a smaller degree, Luczak 2006), the DLA-based model makes it
 164 possible to generate 3D structures similar to different types of dendritic and axonal

trees (Fig. 3; Table 2 in Luczak 2006 provides detailed comparison of dendrite geometry parameters for generated and actual neurons which were obtained from <http://neuromorpho.org>, Ascoli et al. 2001).

4 Estimating the Effect of Environmental Variables on Neuronal Shape

Modeling neuronal growth can provide information on which environmental factors may be influencing neuronal shape. Moreover, it was proposed in (Luczak 2010), that modeling can also be used to infer what environmental conditions for any actual reconstructed neuron were. By measuring “how easy” it is to reproduce the shape of the actual neuron with the appropriate model, it can be estimated how “typical” the neuron is, and which environmental variables have to be adjusted to better reproduce it. For example, if increasing the concentration of NPs in the upper part of the box results in a model that can “easier” or “better” reproduce a given neuronal tree, then it may indicate that this neuron experienced more neurotrophic factors in upper cortical layers.

As an example of how to measure “how easy” it is to reproduce a neuron with a DLA-based model, let’s use the DLA algorithm with uniform distribution of NPs as described in details in (Luczak 2010). The “reproduction” rules are similar to rules generating DLA. The algorithm starts by placing the seed particle at the location of the cell body of the reproduced neuron (Fig. 4a). Randomly moving particles (NPs) stick irreversibly at the first point of contact with the aggregate only if the point of that contact overlaps with a reproduced object (Fig. 4b). By definition, every particle at the time of connecting to the aggregate has a hit value equal to 1. Moving particles which contact the aggregate at the point not overlapping with the object are not connected (Fig. 4c, particle on the right side). If such a moving particle in the next step moves to a place already occupied by the aggregate, then that particle is deleted, and the aggregate at that point registers a new hit (Fig. 4d). In summary, the aggregate grows at the points of contact with randomly moving particles, covering the reproduced neuron particle-by-particle.

Thus, a randomly moving particle after hitting the aggregate will either become a new particle of the aggregate, or it will be deleted depending on whether or not the place of contact overlaps with the reproduced shape. To illustrate how many times a particle of the reproduced neuron was hit by moving particles during the growth process, a sample pyramidal neuron and Purkinje cell are color-coded for the total number of hits (Fig. 4e, f). As can be seen just by visual inspection, the distribution of hits will be different for both cell types. For pyramidal cell most branches were hit a similar number of times. In contrast, for Purkinje cell the number of hits decreased gradually with distance from the soma. One could measure distance between hit distributions for analyzed objects to evaluate similarity between them. For example, comparing the hit distribution of an analyzed structure to the

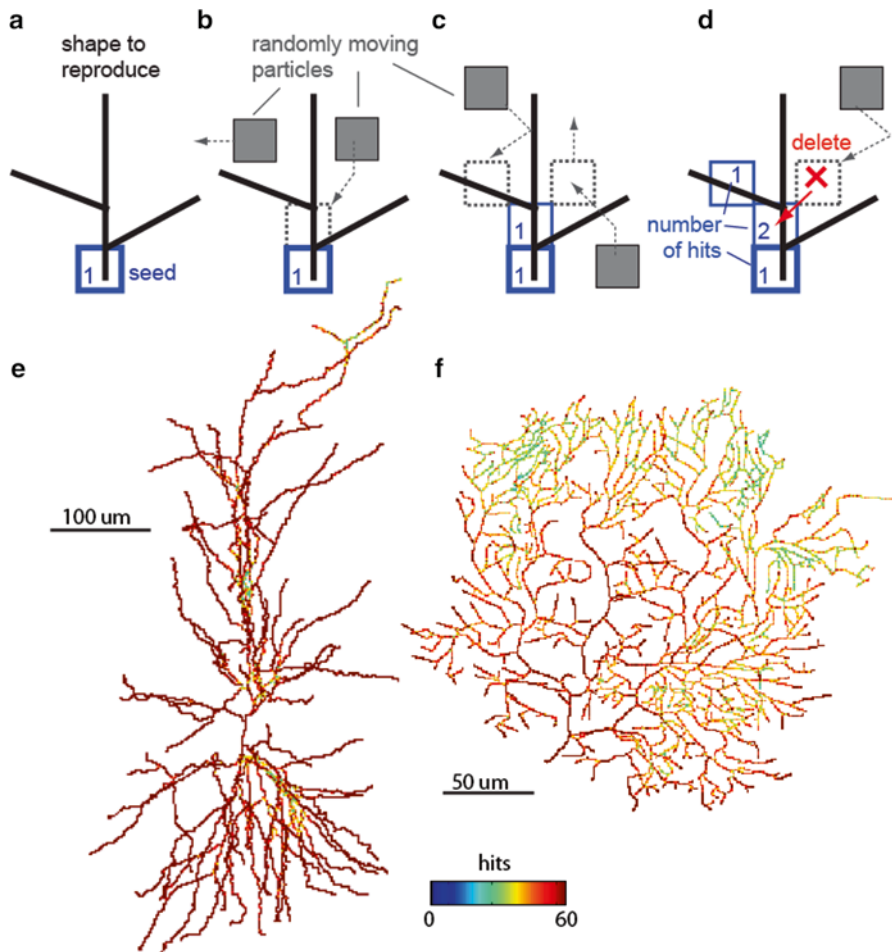


Fig. 4 Reproduction of neuronal shape with the DLA algorithm. (a) To reproduce the given shape, first the initial particle (seed) is placed as the origin of the aggregate. (b) Randomly moving particles (grey) stick to the aggregate at the place of contact, forming new particles of the aggregate (blue). (c) Particles which contact the aggregate at places which do not overlap with the reproduced shape are not connected to the aggregate (right side particle). (d) If the particle moves at the place already occupied by the aggregate, this particle is deleted (red cross). Numbers illustrate how many particles moved over (hit) that place of the aggregate—this number is called the number of hits. (e) Examples of pyramidal cell reproduced in 3D. Color denotes the number of “hits” each part of the dendrite received. (f) Reproduced Purkinje cell (modified from Luczak 2010)

205 distribution of hits for a structure generated with a DLA algorithm, it could provide
 206 a reliable measure for how similar to a typical DLA structure (“DLA-like” or
 207 “tree-like”) is a given shape (Luczak 2010). Likewise, using a DLA-based model
 208 optimized to generate specific type of neurons (as described in Sect. 3) could be

[AU1]

used to measure, for example, how similar to typical Purkinje cell is an analyzed neuron, and it can be further used to infer what parameters reflecting environmental conditions have to be adjusted to improve the reproduction.

5 Discussion

The main significance of the presented model is that it illustrates that the creation of complex dendritic trees does not require precise guidance or an intrinsic plan of the neuron geometry, but rather, that external factors can account for the spatial embedding of the major types of dendrites observed in the cortex. In this model, the number of terminal branches, the mean and maximum branch orders, the fractal dimension, and other parameters of dendrite geometry are all controlled by a few basic environmental factors (Luczak 2006). The most important factor in determining the shape of generated neurons is the space available for growth and the spatial distribution of NPs. Thus, the presented DLA-based model reveals that a simple, diffusive growth mechanism is capable of creating complex and diverse 3D trees strictly similar to observed neuronal shapes.

[AU2] The main criticism of this model is that although it is able to generate diverse neuronal shapes, a direct translation to biological processes is difficult, as real dendrites do not grow directly by aggregating particles from their environment (van Ooyen 2011). This is a very important point, but with a closer examination it can be found that the presented model is much less artificial than it would appear. This is because in the DLA model, connecting a new particle to the aggregate is computationally equivalent to the growth in the direction of that particle. DLA is an approximation of Laplacian growth where the probability of growth at any point on the boundary of the growing object is determined by Laplace's equation, which describes the "attraction" field around the object (Hastings and Levitov 1998). Therefore, the growth in the direction of a local gradient is computationally equivalent to the DLA model which connects particles to the aggregate with higher probability in places which have higher local concentration of NPs. Thus, DLA is used as a computationally convenient tool to model (1) the growth of a dendrite toward a higher concentration of NPs, (2) diffusive motion of NPs, and (3) competition between dendrites for access to NPs.

The real dendrites grow by elongation and can branch either via bifurcation of growth cone-like tips or through interstitial sprouting of new branches from an existing dendritic branch. These new branches extend and retract to undergo constant remodeling. Only a subset is eventually stabilized (Jan and Jan 2003). This phenomenon of constant pruning of dendritic branches during neuron development is modeled here by probabilistic deleting the terminals. Parts of the neuron, which were not deleted during a specified number of iteration (pruning span), become "stabilized" by being excluded from any further pruning. The growth and pruning of real cortical neurons is strongly influenced by the excess or deficit of extrinsic factors, which includes for example: neurotrophin 3, brain-derived

250 neurotrophic factor (BDNF), and nerve growth factor (McAlister et al. 1997).
251 For instance, BDNF released from an individual cell alters the structure of nearby
252 dendrites on an exquisitely local scale (Horch and Katz 2002). The intrinsic factors
253 have an effect on stability rather than the directionality of the dendrite by affecting
254 the dynamics of the structural components of dendrites (Scott and Luo 2001). The
255 NPs in the presented model do not refer to any concrete neurotrophic substance. We
256 chose to call these particles “neurotrophic” to suggest a biological interpretation of
257 the model, which is that a new dendrite branch sprouts at the point of contact with
258 neurotrophic particles. Stated differently, connecting NP to the aggregate can be
259 seen as equivalent to the process where a new part of a dendrite comes from the cell
260 itself at the location where the NP was detected. Also, a decrease in the number of
261 freely moving NPs after contacting the aggregate has a biological justification,
262 namely, that the neurotrophic molecules are commonly uptaken by neurons and
263 transported to the cell body (Purves 1988; von Bartheld et al. 1996). As mentioned
264 above, the neuron development is a very complicated process and the model pre-
265 sented here cannot account for all possible phenomena affecting neuron shape. For
266 example, the morphology of axons and dendrites can be affected by mechanical
267 tensions during brain development (Van Essen 1997). Additional model parameters
268 could improve the model’s accuracy, but would also increase its complexity. Thus,
269 in light of the fact that the existing model performs well, at the goal of keeping the
270 model simple, we believe the model’s current level of complexity and accuracy are
271 appropriately balanced.

272 The presented DLA-based model can also be used to infer parameters describ-
273 ing environmental factors for a given actual neuron. It is a conceptually new
274 approach based on measuring “how easy” it is to reproduce neuronal shape by
275 using a tree-generating algorithm. Thus, by finding what values of environmental
276 variables allow the model to “best” reproduce of the analyzed neuron, it could
277 provide information about conditions shaping this neuron. Performance of DLA
278 algorithms could be measured in a variety of ways: for example, how quickly it
279 can cover shape, how completely it covers, how broad the distribution of hits is.
280 From all of the different measures tried, the distance to the hit distribution of DLA
281 provided the most reliable measure of similarity to modeled shape. In addition,
282 taking for example the model optimized for generating Purkinje cells, and meas-
283 uring how well this model can reproduce given shape, this can provide a new
284 measure of shape, i.e., how “Purkinje-like” is that object. There is still no single
285 measure which quantifies our intuitive perception of how much this cell resembles
286 a Purkinje neuron. This type of question is easily answered by humans, but it is
287 very difficult to quantify using computers. The reason is that perception of a tree-
288 like shape requires simultaneously combining a multitude of global and local
289 measures like spatial distribution of segments, relative lengths and direction, con-
290 nectivity, symmetry, space filling, etc. For example, we would consider as a tree
291 only shapes with a particular type of connectivity pattern, and with a particular
292 spatial distribution of segments, branching angles, relative lengths, orientation,
293 etc. By using the DLA model to reproduce analyzed objects, we can quantify the
294 tree-like resemblance of an object by simply measuring performance of the DLA
295 algorithm. Thus, this approach presents a new conceptual advancement where the

use of a computational model allows one to assess complex properties of an object, 296
 which otherwise would be very difficult to quantify with any other existing 297
 measures. 298

In conclusion, this chapter describes a realistic model of the formation of diverse 299
 neuron shapes. The results demonstrate that simultaneously grown diffusion- 300
 limited aggregates competing for available resources create reproducible, self- 301
 organized structures that are strikingly similar to real neurons (Fig. 3). This is the 302
 first model to simulate 3D neuronal growth accounting for external factors such as 303
 the NP concentration, competition between neurons, and space limitations. 304
 Moreover, it advances DLA-based models by incorporating pruning and space 305
 limitations. Analysis of the discrepancies between generated and real neurons may 306
 also elucidate the relative contribution of different environmental factors on neuro- 307
 nal outgrowth. 308

Acknowledgments This work was partly supported by grants from NSERC and AHFMR. 309

[AU3] **References** 310

Amirikian B (2005) A phenomenological theory of spatially structured local synaptic connectivity. 311
 PLoS Comput Biol 1:74–85 312
 Ascoli GA (1999) Progress and perspectives in computational neuroanatomy. *Anat Rec* 313
 257:195–207 314
 Ascoli GA (2002) Neuroanatomical algorithms for dendritic modeling. *Network* 13:247–260 315
 Ascoli GA, Krichmar J, Nasuto S, Senft S (2001) Generation, description and storage of dendritic 316
 morphology data. *Philos Trans R Soc Lond B Biol Sci* 356:1131–1145 317
 Brady R, Ball R (1984) Fractal growth of copper electrodeposits. *Nature* 309:225–229 318
 Burke RE, Marks WB (2002) Some approaches to quantitative dendritic morphology. In: Ascoli 319
 GA (ed) *Computational neuroanatomy: principles and methods*. Humana, Totowa, NJ, 320
 pp 27–48 321
 Cuntz H, Forstner F, Borst A, Häusser M (2010) One rule to grow them all: a general theory of 322
 neuronal branching and its practical application. *PLoS Comput Biol* 6:e1000877 323
 Devries SH, Baylor DA (1997) Mosaic arrangement of ganglion cell receptive fields in rabbit retina. 324
J Neurophysiol 78:2048–2060 325
 Family F, Platt DE, Vicsek T (1987) Deterministic growth model of pattern formation in dendritic 326
 solidification. *J Phys A* 20:1177–1183 327
 Halsey TC (1990) Electrodeposition and diffusion-limited aggregation. *J Chem Phys* 328
 92:3756–3767 329
 Halsey TC (1997) The branching structure of diffusion limited aggregates. *Europhys Lett* 39:43–48 330
 Hastings MB, Levitov LS (1998) Laplacian growth as one-dimensional turbulence. *Physica D* 331
 116:244–250 332
 Hentschel HGE, Fine A (1996) Diffusion-regulated control of cellular dendritic morphogenesis. 333
Proc R Soc Lond B 263:1–8 334
 Horch HW, Katz LC (2002) BDNF release from single cells elicits local dendritic growth in nearby 335
 neurons. *Nat Neurosci* 5:1177–1184 336
 Jan YN, Jan LY (2010) Branching out: mechanisms of dendritic arborization. *Nat Rev Neurosci* 337
 11:316–328 338
 Koene RA, Tijms B, van Hees P, Postma F, de Ridder A, Ramakers GJ, van Pelt J, van Ooyen A 339
 (2009) NETMORPH: a framework for the stochastic generation of large scale neuronal 340
 networks with realistic neuron morphologies. *Neuroinformatics* 7(3):195–210 341

- 342 Krichmar JL, Nasuto SJ, Scorcioni R, Washington SD, Ascoli GA (2002) Effects of dendritic
343 morphology on CA3 pyramidal cell electrophysiology: a simulation study. *Brain Res*
344 941:11–28
- 345 Lindsay KA, Maxwell DJ, Rosenberg JR, Tucker G (2007) A new approach to reconstruction
346 models of dendritic branching patterns. *Math Biosci* 205:271–296
- 347 Luczak A (2006) Spatial embedding of neuronal trees modeled by diffusive growth. *J Neurosci*
348 *Methods* 157(1):132–141
- 349 Luczak A (2010) Measuring neuronal branching patterns using model-based approach. *Front*
350 *Comput Neurosci* 4:135
- 351 Mainen ZF, Sejnowski TJ (1996) Influence of dendritic structure on firing pattern in model neocortical
352 neurons. *Nature* 382:363–366
- 353 McAlister AK, Katz LC, Lo DC (1997) Opposing roles for endogenous BDNF and NT-3 in regulat-
354 ing cortical dendritic growth. *Neuron* 18:767–778
- 355 Migliore M, Cook EP, Jaffe DB, Turner DA, Johnston D (1995) Computer simulations of morpho-
356 logically reconstructed CA3 hippocampal neurons. *J Neurophysiol* 73:1157–1168
- 357 Niemeyer L, Pietronero L, Wiesmann HJ (1984) Fractal dimension of dielectric breakdown. *Phys*
358 *Rev Lett* 52:1033–1036
- 359 Nowakowski RS, Hayes NL, Egger MD (1992) Competitive interactions during dendritic growth:
360 a simple stochastic growth algorithm. *Brain Res* 576:152–156
- 361 Perin R, Berger TK, Markram H (2011) A synaptic organizing principle for cortical neuronal
362 groups. *Proc Natl Acad Sci U S A* 108:5419–5424
- 363 Purves D (1988) *Body and brain. A trophic theory of neural connections.* Harvard University
364 Press, Cambridge, MA
- 365 Samsonovich AV, Ascoli GA (2003) Statistical morphological analysis of hippocampal principal
366 neurons indicates cell-specific repulsion of dendrites from their own cells. *J Neurosci Res*
367 71:173–187
- 368 Samsonovich AV, Ascoli GA (2005) Statistical determinants of dendritic morphology in hippo-
369 campal pyramidal neurons: a hidden Markov model. *Hippocampus* 15:166–183
- 370 Scott E, Luo L (2001) How do dendrites take their shape? *Nat Neurosci* 4:353–359
- 371 Stepanyants A, Chklovskii DB (2005) Neurogeometry and potential synaptic connectivity. *Trends*
372 *Neurosci* 28:387–394
- 373 Torben-Nielsen B, Vanderlooy S, Postma EO (2008) Non-parametric algorithmic generation of
374 neuronal morphologies. *Neuroinformatics* 6(4):257–277
- 375 Van Essen DC (1997) A tension-based theory of morphogenesis and compact wiring in the central
376 nervous system. *Nature* 385:313–318
- 377 Van Ooyen A, Graham B, Ramakers G (2001) Competition for tubulin between growing neurites
378 during development. *Neurocomp* 38–40:73–78
- 379 Van Pelt J, Dityatev A, Uylings HBM (1997) Natural variability in the number of dendritic seg-
380 ments: model-based inferences about branching during neurite outgrowth. *J Comp Neurol*
381 387:325–340
- 382 Van Pelt J, Uylings HBM, Verwer RWH, Pentney RJ, Woldenberg MJ (1992) Tree asymmetry – a
383 sensitive and practical measure for binary topological trees. *Bull Math Biol* 54:759
- 384 Von Bartheld CS, Williams R, Lefcort F, Clary DO, Reichardt LF, Bothwell M (1996) Retrograde
385 transport of neurotrophins from the eye to the brain in chick embryos: roles of the p75NTR and
386 trkB receptors. *J Neurosci* 16:2995–3008
- 387 Voss RF (1984) Multiparticle fractal aggregation. *J Stat Phys* 36:861–872
- 388 Witten TA, Sander LM (1981) Diffusion limited aggregation, a kinetic critical phenomena. *Phys*
389 *Rev Lett* 47:1400–1408
- 390 Zubler F, Douglas R (2009) A framework for modeling the growth and development of neurons
391 and networks. *Front Comput Neurosci* 3:25